Dynamics and microrheology of colloidal clay-polymer glasses and gels: Size-dependent phenomena and re-entrant behavior at early aging times

Jiachun Shen, Surita R. Bhatia*

¹Department of Chemistry, Stony Brook University, Stony Brook, NY 11794-3400 USA *Corresponding author, <u>surita.bhatia@stonybrook.edu</u>

Abstract

The colloidal clay Laponite forms a variety of arrested states that display interesting aging behavior. Microrheology has been applied to Laponite-based glasses and gels, but few studies evaluate the influence of probe particle size. In this work, we report the dynamics and microrheology of Laponite-polymer dispersions during aging, using passive microrheology with three different probe particle sizes. At early aging times, the neat Laponite dispersion forms an arrested state; the nature of this state (e.g. a repulsive glass or gel) has remained the subject of debate. The addition of polymer retards the gelation and melts the arrested state. While this melting has been observed at the macroscale and has been attributed to a re-entrant transition of a repulsive glass to a liquid state, to our knowledge it has not been observed at the microscale. The delay of the gelation time needed to form an arrested state was found to depend on the polymer concentration and could vary from ~24 h for neat Laponite to 7 days for some Laponite-polymer samples. Significant effects of probe particle sizes are observed from the mean-squared displacement (MSD) curves, as small and intermediate probe particles show diffusive motion, while the motion of large particles is restricted. By examining the factor $\langle \Delta r^2(\tau) \rangle a$, structural heterogeneity can be confirmed through the strong size-dependence displayed. Different MSD trends of probe particles are obtained at longer aging times, but no significant changes occur after 30 days of aging. Our microrheology results also reveal significant effects of probe particle size.

Introduction

Colloidal dispersions have been extensively investigated in recent decades due to their wide existence in nature and range of applications in industry. Colloidal suspensions have various applications such as coatings, polymer-clay nanocomposites, and cosmetics.¹⁻³ Colloidal dispersions are known to experience a variety of different dynamically arrested states due to interparticle interactions, which have stimulated numerous fundamental studies of phase behavior and dynamics of colloidal glasses and gels. ⁴⁻⁸ It was found that the formation and structure of these arrested states could be controlled by multiple factors including ionic strength, solution pH, and the addition of additives like non-adsorbing or adsorbing polymers.⁹⁻¹² The phase diagram and structural dynamics of gels and glasses of a specific class of colloids, discotic colloidal clays, have been a subject of intense debate and discussion.

Among the most investigated colloidal clay particles, the synthetic clay Laponite has received tremendous interest due to its applications and various arrested states at different conditions. ^{10, 13} Laponite is a synthetic colloidal platelike particle, about 25 nm in diameter and 1 nm in thickness, and the corresponding reduced molecular formula is Na⁺0.7[Si₈Mg_{5.5}Li_{0.3}O₂₀(OH)₄]⁻0.7. Laponite particles carry permanent negative charges on each face of the disk due to isomorphic substitution and possess pH-dependent charges on the edges. It is reported that the isoelectric point of the edges is about pH =11.¹⁴ The edges are positively charged at lower pH, and negative charges are dominant at pH > 11. Although edges may still have some localized positive charges at pH = 10-11, the repulsive interaction dominates in the aqueous dispersions in this pH range, leading to the formation of an arrested state without the addition of electrolytes. At lower pH, positive changes on the edge are present, leading to an edge-to-face attraction that is responsible for the structural arrest driven by aggregation and gelation. 11, 15 Additionally, the particle orientation caused by electrostatic interactions can be tuned and controlled by the ionic strength I in the dispersion, which affects the formation of the electrical double layer.¹⁴ Adding electrolytes into the dispersion increases the ionic strength and screens the repulsive force between clays, leading to the emergence of attractive interactions and the formation of either gel states or attractive glasses. ^{6,11,16,17} Thus, adjustment of the pH and the addition of electrolytes significantly influence the arrested states and the related structural and rheological properties.

The nature of arrested states and aging behavior of Laponite dispersions have also been found to be dependent on the particle and additive concentrations. When stored over time, Laponite dispersion evolves from a viscous liquid-like state to a nonergodic arrested state. In previous studies, Laponite dispersions were observed to display a transition from a liquid state to an arrested state; some authors have characterized this state as a repulsive glass driven by repulsive interaction between edges or faces, while others have characterized it as a gel. ^{15, 18} The dynamics and evolution of Laponite dispersions at various concentrations during the aging process have been widely investigated using dynamic light scattering

(DLS), small-angle X-ray scattering (SAXS), and numerical simulations combined with rheological analysis. ^{5, 10, 19-23} The interaction and structural evolution of Laponite can also be tuned by the addition of electrolytes and polymers, where heterogeneous structures are found in the dispersion and significant changes are observed during the aging process. It was reported that a shorter aging time was required for the formation of the arrested state with the addition of salts as compared to the neat Laponite dispersion. ²⁴

However, the addition of polymer to the Laponite dispersion changes the particle interactions and can influence aging in a different manner. In the presence of polymers that do not adsorb onto the clay surface, the original arrested state melts and remains as a viscous fluid, while the influence of adding absorbing polymers strongly depends on the molecular weight of polymers. 19, 25, 26 In our previous work, Baghdadi et al. studied the effects of different molecular weights of an adsorbing polymer, poly(ethylene oxide) (PEO), on Laponite dispersion, and found that the low molecular weight PEO ($M_n \le 60$ kg/mol) acts to melt the arrested state of Laponite. This was proposed to be due to a depletion attraction from free chains that are present when the polymer concentration is above the saturation concentration of the clay surfaces.²⁷ When it comes to higher molecular weight PEO ($M_n > 83$ kg/mol), the dispersion forms an attractive gel state with the polymer chain bridging between clay particles to facilitate the formation of viscoelastic solids. At sufficiently high polymer concentrations, even if the polymer chains are too short to bridge between particles, an arrested state is also formed, presumably because the depletion attractions become strong enough to form an attractive gel. This re-entrant phase behavior, observed via bulk rheology, has been described in previous studies.²⁷⁻²⁹

The dynamics and aging behavior of Laponite dispersions has previously been studied by microrheology³⁰; however, most studies have utilized only one probe particle size (dispersed particles or added tracers). There has been some work to compare the size dependence of probe dynamics in polymer or colloidal gels,³¹⁻³³ however further study of any size-dependent effects on the aging of colloidal clay dispersion is warranted. Additionally, few microrheology studies have been carried out on Laponite/polymer systems and the various types of arrested and re-entrant states displayed by these materials.

In this work, we study the structural evolution and rheological aging of Laponite dispersions with different PEO concentrations through passive DLS-microrheology, tracking the thermal motion of embedded probe particles with various sizes. A fixed 2 wt% clay concentration with a broad range of PEO content (0-2.5 wt%) is explored using three different probe particle sizes (65 nm, 480 nm, and 2000 nm). Different aging times are recorded to analyze the evolution of arrested states and viscoelastic properties. The pH of the Laponite dispersion is adjusted to 10 to be in the range where the neat Laponite dispersion is expected to form a colloidal glass, with repulsive interparticle interactions being dominant. Distinct aging processes are observed for different PEO concentrations, resulting in different gelation times and arrested states. Significant effects of probe particle sizes are confirmed by comparing the mean-squared displacement (MSD) of tracers and the corresponding microrheological viscoelastic moduli, suggesting that some of the

observed behaviors are due to confinement of probe particles and the length scale of structural heterogeneities in the glasses and gels.

Materials and Methods

Laponite® RD was obtained from Southern Clay Products (Gonzales, TX). Poly(ethylene glycol) (PEO, M_n : 20000 g/mol) was purchased from Sigma (USA). Sodium hydroxide and hydrochloric acid were obtained from Fisher Scientific (USA). Carboxyl polystyrene latex (4%, w/v) with different nominal diameters were purchased from Thermo Fisher Scientific (USA), which are named as 65 nm, 480 nm, and 2000 nm. The average effective diameters measured by dynamic light scattering (DLS) are 66 ± 1 nm, 518 ± 7 nm, and 1945 ± 25 nm, respectively. Deionized water was used to prepare all samples. All chemicals were used without any further purification or treatment.

Sample preparation

To prepare 2 wt% Laponite dispersions, specific amounts of clay powder were added to deionized water of pH =10 (adjusted by adding 0.1 mol/L NaOH and HCl solutions as needed). The resulting dispersion was stirred at a constant stirring rate for 1 h to fully disperse clay particles in the solution. For the Laponite/PEO samples, the necessary amounts of PEO powder were added into the Laponite dispersion and then the dispersion was mixed by stirring for 1 h to obtain the stock dispersion of 2 wt% Laponite and 2.5 wt% PEO. For the series of Laponite/PEO dispersions, the desired amount of pure 2 wt% Laponite dispersion was mixed with the stock Laponite/PEO dispersion to obtain the diluted dispersion of 0.25-2.25 wt% PEO with 2 wt% Laponite. Samples are named LxPEOy based on the concentration of components, where x represents the concentration in wt% of Laponite and y represents that of PEO, e.g., L2PEO1.25 for a dispersion of 2 wt% Laponite and 1.25 wt% PEO. About 3 mL of each obtained dispersion was transferred into a plastic cuvette and one drop of solutions containing carboxyl polystyrene particles (about 0.05 wt%) was added to each sample to serve as probe particles. For each concentration of PEO, three samples were prepared and three sizes of probe particles (65 nm, 480 nm, and 2000 nm) were added to the samples, respectively. All the cuvettes were capped and stored in a drawer at room temperature. We consider aging time t = 0 to be the time when these cuvettes were stored in the drawer. Dilution experiments for Laponite/polymer samples with higher PEO concentrations were conducted after long aging times to confirm the gel-like state instead of repulsive glassy state (results not shown).

Microrheological measurements

Microrheological measurements of Laponite/PEO dispersion were performed on the NanoBrook Omni instrument (Brookhaven Instrument Inc., Holtsville, NY) with a 650-nm diode laser. All measurements were carried out with 3 repeats at 25 °C. Because the samples are non-ergodic, multiple measurements were performed for each sample while varying the position of the cuvette; three measurements were made in each of four different

positions, for a total of 12 measurements per sample. Samples were measured after 1 day, 7 days, 30 days, 42 days, and 60 days of aging at room temperature. Measurements of some samples at the longer aging time were not reported due to the unexpected solvent evaporation or high signal-to-noise ratio.

DLS-Microrheology

To measure the microscale viscoelasticity of the system, the probe particle was added to the dispersion and the thermally activated Brownian motion was calculated by detecting the scattered intensity of the probe particle and applying the generalized Stokes-Einstein relation (GSER). The ensemble-averaged mean squared displacement (MSD) is calculated as follows:

$$\langle \Delta r^2(\tau) \rangle = \langle |r(t+\tau) - r(\tau)|^2 \rangle \tag{1}$$

For a spherical particle in a Newtonian fluid of viscosity η with radius a, the MSD is also related to the diffusion coefficient D via

$$\langle \Delta r^2(\tau) \rangle = 2dD\tau \tag{2}$$

$$D = \frac{k_B T}{6\pi \eta a} \tag{3}$$

where d is the dimensionality of measurement, τ is the lag time, k_B is the Boltzmann constant and T is the temperature.

The frequency-dependent complex modulus G^* (ω) can be obtained from the Fourier transform of MSD by GSER:

$$G^*(\omega = 1/\tau) = \frac{k_B T}{\pi a i \omega \mathcal{F}\{\langle \Delta r^2(\tau) \rangle\}}$$
 (4)

where $\mathcal{F}\{\langle \Delta r^2(\tau) \rangle\}$ is the Fourier transformed MSD and ω is the frequency.³⁴ The storage modulus (G') and loss modulus (G") of the complex material could be obtained by the following relations:

$$G' = |G^*(\omega)| * \cos\left(\frac{\pi\alpha(\omega)}{2}\right)$$
 (5)

$$G'' = |G^*(\omega)| * \sin\left(\frac{\pi\alpha(\omega)}{2}\right)$$
 (6)

where

$$|G^*(\omega)| \approx \frac{k_B T}{\pi a \langle \Delta r^2(\frac{1}{\omega}) \rangle \Gamma[1 + \alpha(\omega)]}$$
 (7)

where Γ is the gamma function due to Fourier transformation.

Results

Before systemically studying the aging behavior of Laponite/PEO samples, the typical aging behavior of pure Laponite samples, probed by a 65 nm tracer, is displayed in Figures 1 a, and 1b, which shows the MSD $<\Delta r^2$ (τ)> curves and the corresponding microscale viscoelastic moduli. Initially, the MSD increases linearly with lag time τ at 2 min aging, and the logarithmic slope of the curve is close to 1, suggesting the motion of the probe particle is near-diffusive over the entire lag time range. As the aging continues, the MSD gradually becomes curved and shows a non-linear trend within 24 h. This indicates that the diffusion of particles becomes retarded and this may be due to the local elasticity of material itself or the potential structural evolution during aging. This will be discussed in further detail in the following section.

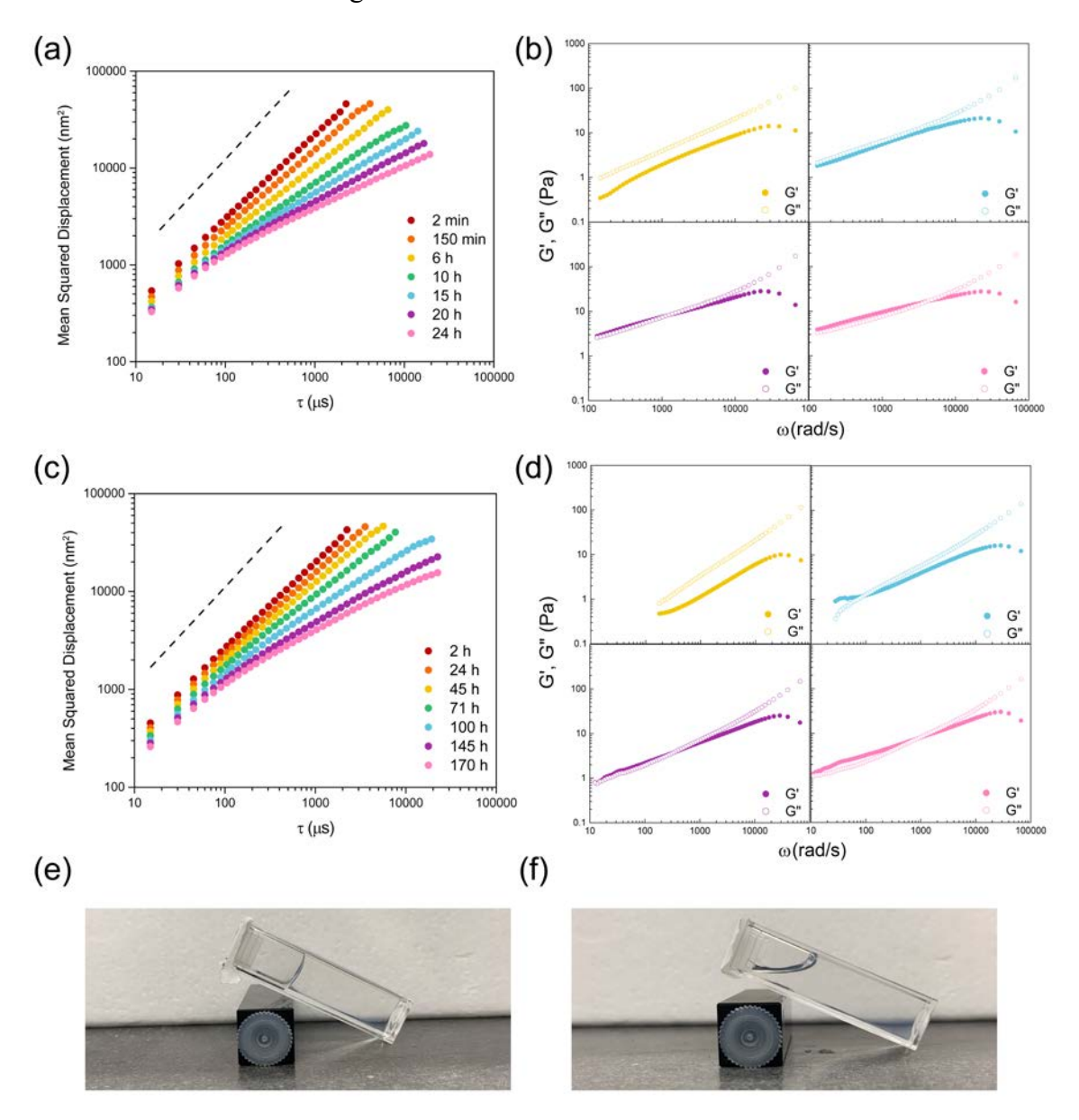


Figure 1. Mean squared displacement of 65 nm probe particle measured by DLS-microrheology in 2 wt% Laponite (a) and 2 wt% Laponite and 1.25 wt% PEO (c) at the

different aging times as indicated. The corresponding microrheological viscoelastic properties calculated from the MSD data shown in (b) and (d), respectively. The colors used in (a) and (c) for the aging times are the same as those used in (b) and (d) to indicate the aging times in the MSD results. Digital images of Laponite (e) and L2PEO1.25 (f) after 1 day of aging. The dashed line in (a) and (c) has a slope of 1.

For the microscale viscoelastic moduli, the loss modulus G" dominates at the early aging time, suggesting an initially viscous state. The storage modulus G' increases at short τ as the sample ages, and it eventually surpasses G" after 20 h, which suggests a transition to an arrested state. As a comparison, a 2.00 wt% Laponite and 1.25 wt% PEO blend sample is also shown, where again the aging behavior has been investigated using a 65 nm probe particle (Figures 1c and 1d). Unlike the pure Laponite sample, the Laponite/PEO sample still shows a linear MSD curve after 24 h, and the particle motion is also near-diffusive. After 145 h of aging, the MSD becomes curved and the crossover point of G' = G'' occurs, revealing that the probe particle's motion is constrained by the surrounding environment. In other words, on the microscale, the Laponite/PEO sample becomes more gel-like after 6 days, as compared to the gelation time of 1 day for the neat Laponite sample. From a macroscopic point of view, after one day of aging, the Laponite sample appears more solid-like, as shown by the digital image (Figure 1e) while a representative Laponite/PEO sample is still in the liquid state (Figure 1f). This implies that the addition of PEO chains into the Laponite system may significantly affect the gelation behavior upon aging.

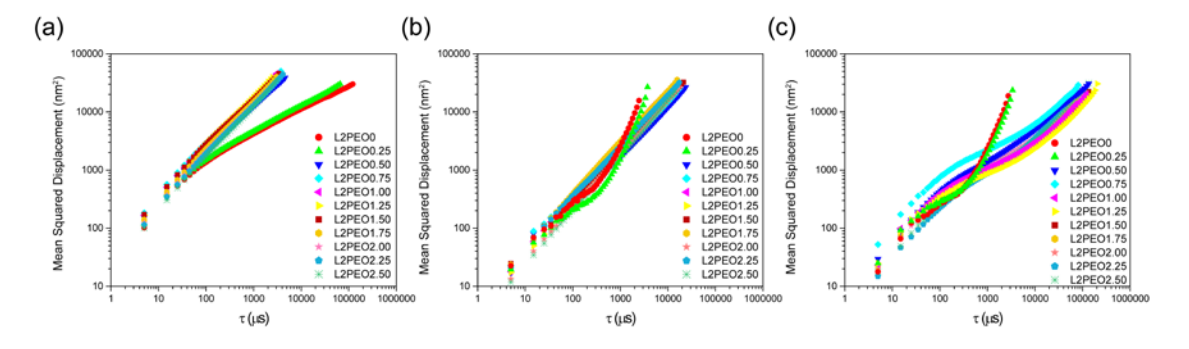


Figure 2. Mean squared displacement in the series dispersions of PEO concentration from 0.00 wt% to 2.50 wt% with a fixed 2 wt% Laponite after 1 day of aging with probe particles of size (a) 65nm, (b) 480 nm, and (c) 2000 nm.

The average MSD curves of Laponite/PEO samples with different probe particle sizes after 1 day of aging are reported in Figure 2. Generally, the samples of pure Laponite and the lowest PEO concentrations (0.25 wt%) showed similar MSD profiles with all three probe particles. As for the small probe particle (65 nm) in Figure 2a, the pure Laponite and 0.25 wt% PEO samples showed non-linear MSD curves, which means the motion of the probe particles was restricted. As we discussed previously, this may be because of the local elastic response or the growing heterogeneity like particle rearrangements in the dispersion. This has been reported in our previous work, and the dispersions are expected to be in the

repulsive colloidal glass state, 18, 27 although as noted above there is also evidence in the literature that this state is a gel rather than a glass. Similarly, the samples at low PEO concentration (0.25 wt%) are also expected to be colloidal glasses; the low concentration of PEO may not be able to affect the particle rearrangement significantly, leading to a similar state as the pure Laponite dispersion. When it comes to medium (480 nm) and large probe particles (2000 nm) in Figure 2b and 2c, the MSD curves became different, showing a linear trend at small τ with a short plateau at medium lag time, followed by a sudden upturn at long lag times. The small plateau with decreasing slopes reveals the probe particle was trapped in the local structure, while the steeply increasing MSD could be due to escape. Compared with 65 nm particle, the small probe particle size limits the length scale it can probe and it may only experience the thermal motion in the same local structure without escape while the intermediate and large size of 480 and 2000 nm particles provide them a chance to escape out of the cage, especially during the initial aging without much aggregation. This also reveals that the constraint from the local structure is not permanent, and the relaxation of constraint allows the probe particles to move more freely at long lag times. The logarithmic slope of this regime is close to 2, which conforms to ballistic motion and could be caused by increasing non-Brownian forces from the local microstructure. 18

For samples with 0.5 wt% and higher concentrations of PEO, the MSD data of the small probe particle (65 nm) depends linearly on the lag time, demonstrating that the Laponite/PEO samples are still in the sol state. This is the same as the medium probe particle (480 nm), which reveals that the tracers can freely diffuse in the local environment. With the large probe particle (2000 nm), the MSD curves showed three different regimes. At the initial stage, the logarithmic slope of MSD is close to 1 and the MSD is dependent on the lag time, which suggests Brownian motion of the probe particle. In the medium time range, the MSD has a much weaker dependence on delay time, with the logarithmic slope much smaller than 1, indicating the restricted motion of probe particles. We refer to this as the constrained regime. In the third regime, the logarithmic slope of the MSD increases again at long lag time, which suggests the probe particle was able to escape from the surrounding medium.

It is worth noting that the addition of PEO (≥0.5 wt%) delays the formation of an arrested state as compared to the neat Laponite dispersion. The Laponite/PEO system is still in a sol state at early aging times and allows the small and medium tracers to move in a viscous local environment. This melting of the glassy states or so-called re-entrant behavior has been found at the macroscale for Laponite-polymer solutions by our group, as well as in other types of colloidal glasses by other researchers. ^{27,29,35,36} In the Laponite-PEO systems, the melting of the repulsive colloidal glass has been attributed to free PEO chains leading to a weak depletion attraction between colloidal particles. Such an interaction moves particles closer and reduces the effective volume fraction, which allows the dispersion to flow. This may lead to the formation of a gel-like state at longer aging times as our previous studies suggest. We note that the radius of gyration of PEO 20k used in this work is calculated as 3.8-7.1 nm based on both theoretical and several empirical formulas ³⁷⁻³⁹ while the theoretical mean interparticle distance of 2 wt% Laponite dispersion is around 40 nm⁴⁰,

 41 . Moreover, our previous work reveals that PEO with molecular weight $\leq 60 \mathrm{k}$ g/mol g/mol will not wrap or form the bridging between the Laponite particles. $^{27, 42}$ Thus, it is believed no significant bridging that affect the structural arrangement will occur between PEO and Laponite particles during the aging in this work. While this type of re-entrant behavior has been observed using macroscale rheology measurements and DLS measurements of the dynamics, to our knowledge it has not been observed using passive microrheology measurements.

As for the large particles (2000 nm), the restricted motion reveals that the size of probe particles may have an influence on probing the local structures as the size of the tracer and the local structure may be comparable, which makes a relative glass-like environment for the tracer. More discussion will be provided in the following section.

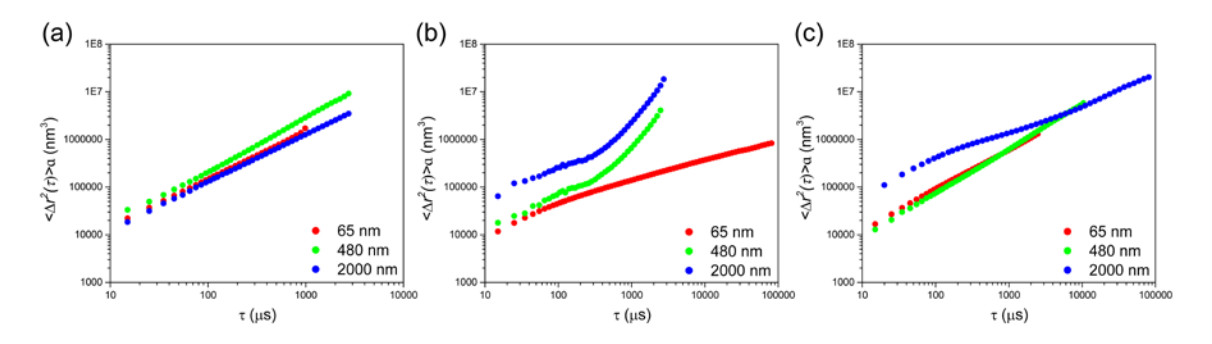


Figure 3. $<\Delta r^2(\tau)>a$ versus lag time of different samples with various probe particle sizes after one day of aging: (a) water, (b) 2 wt% Laponite, and (c) 2 wt% Laponite and 1.50 wt% PEO.

It was previously reported that the plateau in MSD curves could be indicative of the local elasticity of the material or the steric constraint from the surrounding pores or cages. $^{31, 33, 43}$ By examining the factor $<\Delta r^2$ (τ)>a, where a is the radius of the probe particle, the product is independent of a if this is due to the elastic response. Otherwise, this is mainly related to the trapping of probe particle in the surrounding cavity. $^{43, 44}$ In Figure 3, the factor $<\Delta r^2$ (τ)>a of selected Laponite and Laponite/PEO sample is plotted as a function of lag time with three different probe particle sizes after 1 day of aging. MSD data for the same probe particles in water are also included. As expected for water (Figure 3a), the $<\Delta r^2$ (τ)>a curve increases linearly and the data for $<\Delta r^2$ (τ)>a overlap well for different probe particles. The curve of the 480 nm particle is slightly higher than the other two curves, but the shape of the MSD is similar, and the small discrepancy may be to any slight error in measured probe particle size.

The same type of analysis on the MSD data for Laponite samples shows different trends. For the pure Laponite sample, the three curves deviate significantly from each other and show no overlap throughout the measurement as shown in Figure 3b. This implies that the

plateau in Laponite sample could be caused by "caging" of probe particles, rather than the material's elasticity. This suggests that the Laponite dispersions have increased in structural heterogeneity, potentially due to particle rearrangements, even after one day of aging. For the 1.25 wt% PEO sample, shown in Figure 3c, the curves of 65 nm and 480 nm particles overlap reasonably up to large τ , but the largest particle shows a different trend and little overlapping with the other two curves. Results for the Laponite/PEO sample suggest that the local elasticity probed by two smaller particles is similar, while the 2000 nm particle provides quite different information on the large length scale. Such large deviations for large probe particles may be ascribed to the relatively large size of the tracers compared to the potential cage size of the dispersion and the limited space for particle diffusion. This implies a strong influence of probe particle size when probing the local environment in microrheology.

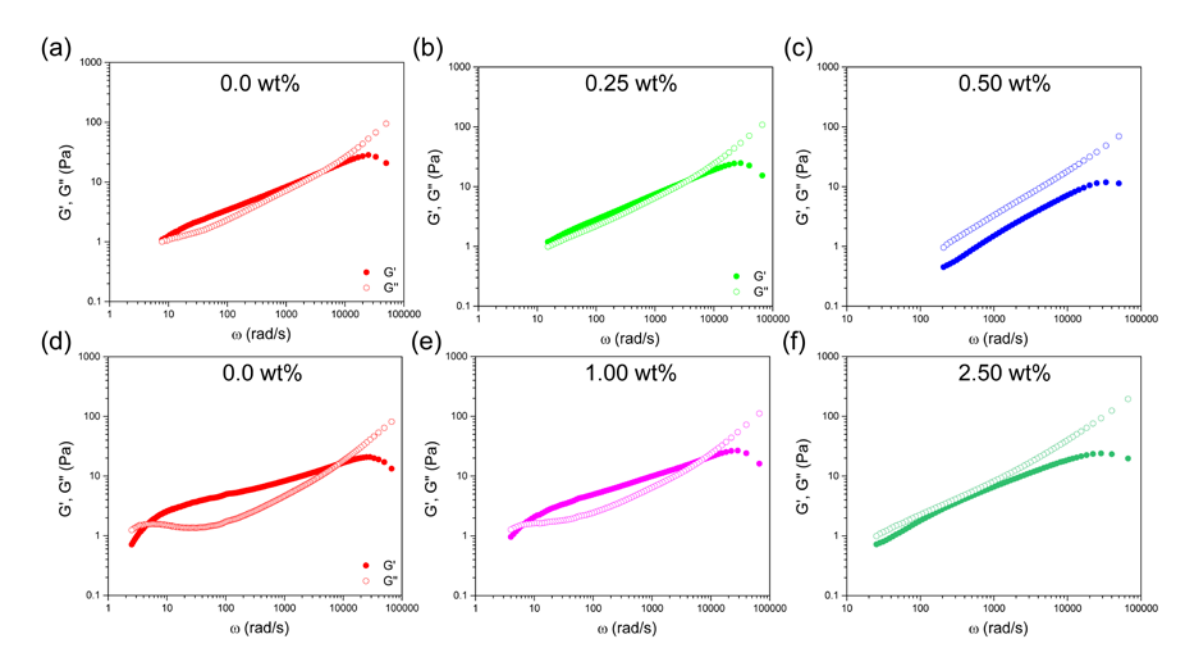


Figure 4. The storage modulus (filled circles) and loss modulus (open circles) calculated from the MSD data for samples with different PEO concentrations at the different aging times as indicated. 1 day of aging (first row): (a) L2PEO0, (b) L2PEO0.25, and (c) L2PEO0.50; 7 days of aging (second row): (d) L2PEO0, (e) L2PEO1.00, and (f) L2PEO2.50.

To monitor the transition from liquid dispersion to arrested state, the frequency-dependent microrheological storage and loss moduli were calculated from the $\langle \Delta r^2(\tau) \rangle$ data using Eq. (5-6). In Figure 4, results of pure Laponite and selected Laponite/PEO samples probed by 65 nm particles are displayed to compare the effect of PEO concentrations on the aging behavior. After 1 day of aging, the pure Laponite and L2PEO0.25 both show G' dominating at intermediate frequencies while G" > G' at high frequencies in Figures 4a and 4b. This is consistent with MSD results that show a non-linear curve, which suggests the L2 and L2PEO0.25 samples have already been in a solid-like state after only one-day aging. As a comparison, samples with 0.5 wt% PEO show a different trend in Figure 4c with G" over

G' throughout the frequencies, indicating a viscous liquid-like state. Samples with higher concentrations of PEO also show a similar profile as G" dominates all over the frequency range (not shown).

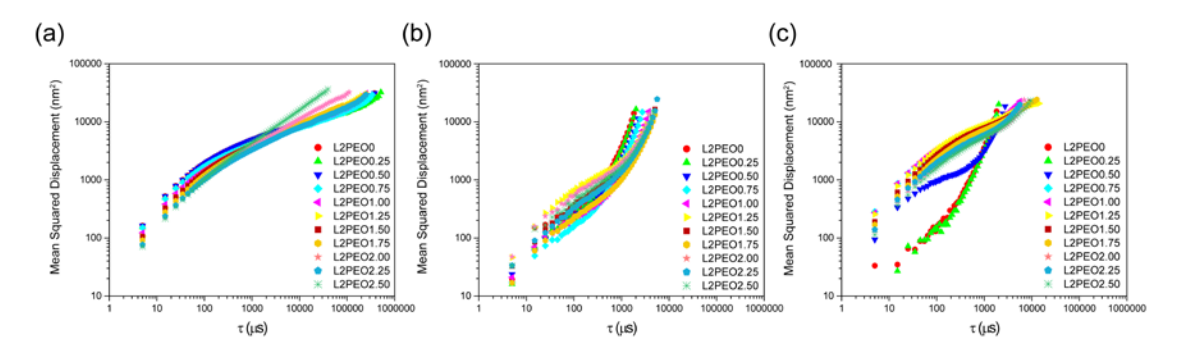


Figure 5. Mean squared displacement of different probe particle sizes in the series dispersions of PEO concentration from 0.00 wt% to 2.50 wt% with a fixed 2 wt% Laponite after 7 days of aging: (a) 65nm, (b) 480 nm, and (c) 2000 nm.

As the aging process continues, the MSD profiles provide more information about the evolution of local structures in the dispersions. Figure 5 shows the average MSD of samples after 7 days of aging. For the 65 nm probe particles in Figure 5a, the MSD data of all the concentrations exhibited a non-linear trend after 7 days of aging, except for the 2.5 wt% samples. As for lower PEO concentrations, the non-linear increase of MSD indicates the restricted motion of probe particles and the increasing hindrance from the occurrence of particle rearrangements inside the dispersion after 7 days of aging time. Compared with the pure Laponite dispersion, the addition of PEO polymer chains significantly delayed the formation of the arrested state until 7 days instead of 1 day while L2PEO2.50 samples are still in a sol state with a linear MSD trend. For the 2.5 wt% sample, more free PEO chains are available in the dispersion which significantly decreases the effective volume fraction and allows for flowing. This is also observed in the change in viscoelastic properties. When it comes to 7 days of aging, both 0.50 wt% and higher PEO concentrations samples show a G' > G" at intermediate frequencies as the profile of 1.00 wt% PEO sample shown in Figure 4e, except for the L2PEO2.50 (Figure 4f). The loss modulus of 2.50% PEO sample increases linearly and is still dominant over the measured range after 7 days of aging. However, the magnitude of G" and G' is so close that the sample is near the critical point as the aging evolution suggests in Figures 1b and 1d. This also reveals that the addition of free polymer chain could significantly affect the clay particle rearrangement and delay the formation of gel-like states. Such a delay of the sol-gel transition increases with the increasing added polymer concentration with the critical time changing from initially less than 24 h to more than 7 days.

Moreover, different MSD trends were observed with the samples containing 480 nm and 2000 nm probe particles (Figures 5b and 5c). For the medium-size probe particle, samples

showed a typical three-regime profile of MSD that includes diffusive, restricted, and superdiffusive motion. This reveals that the probe particle experienced a free movement at first and was then trapped in the cage with escape at long lag time. Samples with large probe particles exhibited different trends with different PEO concentrations. In detail, the pure Laponite and 0.25 wt% samples have the similar MSD trend to that of 1 day of aging, which increases linearly at small τ and shows a sudden upturn after that. 0.75 wt% and higher concentration samples showed a long range of plateau at intermediate lag time and a short regime at large τ with increasing logarithmic slope while the 0.50 wt% sample experienced a three-regime profile with an early plateau and lower MSD values. It is speculated that the 0.50 wt% sample is close to the critical concentration that transits to the repulsive glass (0.00 wt% and 0.25 wt%) or the arrested gel with the adsorption of PEO on Laponite particles (0.75 wt% and higher), which may lead to such a different MSD trend between two different profiles.

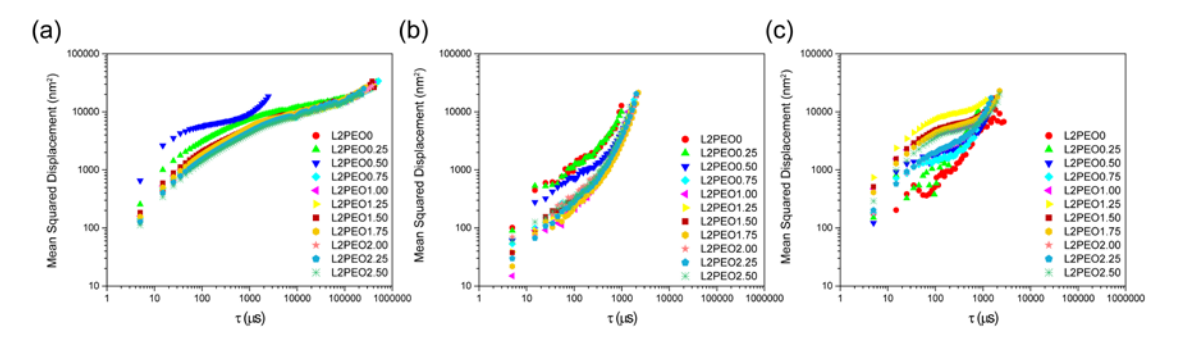


Figure 6. Mean squared displacement of different probe particle sizes in the series dispersions of PEO concentration from 0.00 wt% to 2.50 wt% with a fixed 2 wt% Laponite after 30 days of aging: (a) 65nm, (b) 480 nm, and (c) 2000 nm. L2PEO0.5 with 65 nm probe particle may be an outlier due to the unknown effects.

As samples were aged for 30 days, all the samples displayed a non-linear dependence on the lag time (Figure 6), which conforms to our previous findings that all the dispersions turned into the arrested state after 28 days. ¹⁸ For 65 nm probe particles in Figure 6a, most samples show curved MSD profiles and experience a plateau at large τ. This reveals that probe particles' motions were restrained and then arrested inside the local structure and were not able to escape from it within the measurement time scale. However, the 0.5 wt% sample showed a distinct MSD trend with an upturn at longer lag time. It is not clear whether there are any defects of sample preparation or other post influences like solvent evaporation that affect the MSD data since it did not follow the trend with the concentration changes. As for the medium probe particles (480 nm) in Figure 6b, only two-regimes were detected and presented for all the samples due to the high noise at long lag time. Basically, samples that underwent diffusive motion at short lag times were suddenly able to run out

of the cage and showed superdiffusive motion due to a non-Brownian force. Large probe particles experience a typical three-regime MSD profile in all the samples, although some data are very noisy. It was observed that there was unexpected evaporation of the solvent in some samples at long aging times, which would cause issues with the data. A representative digital picture of such a sample is shown in Supplemental Information Figure S4. The gel sample shrinks, with traces attached to the wall of cuvette, indicating the change in height of gel and movement of gel-air interface. Considering no significant mechanical motion has been applied to samples, we believe this is mainly due to the evaporation of water. Such significant change in macroscale could also influence the structure of samples in microscale, which results in inconsistent data in measurements.

Aging behavior at longer time (42 days and 60 days) are also evaluated by DLS-microrheology and shown in Supplementary Information Figure S1. Generally, the trend of MSD data with different probe particles is consistent with the 30-day data, and there is not much change in MSD values. It appears that sample aging slows down and most structural evolution occurs within 30 days. Thus, our analysis and discussion will mainly focus on samples in the first 30 days of aging.

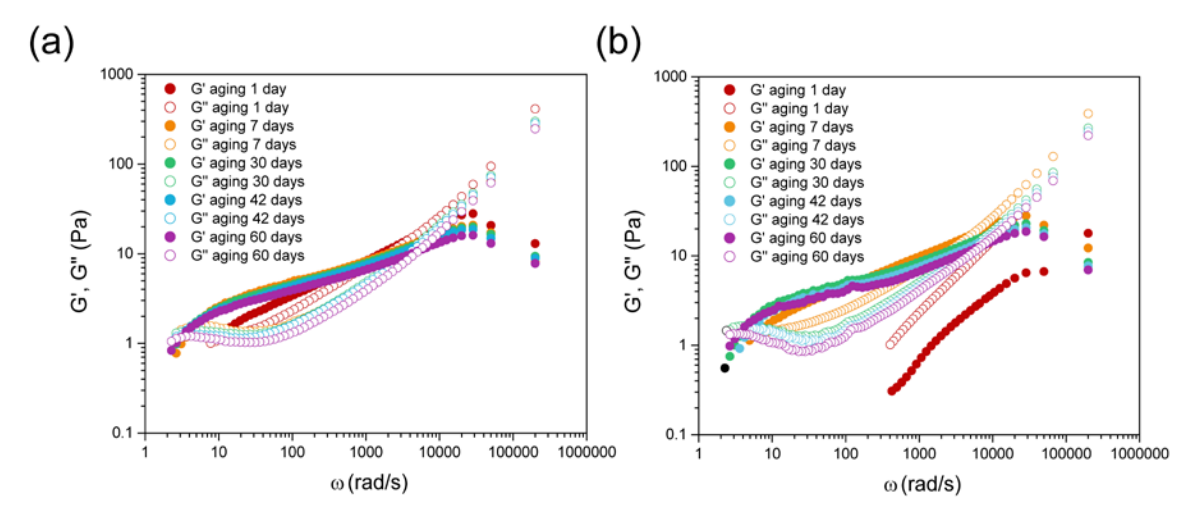


Figure 7. The storage modulus (filled circles) and loss modulus (open circles) calculated from the MSD data for representative samples with 65 nm probe particle at different aging times as indicated: (a) L2PEO0, (b) L2PEO1.25.

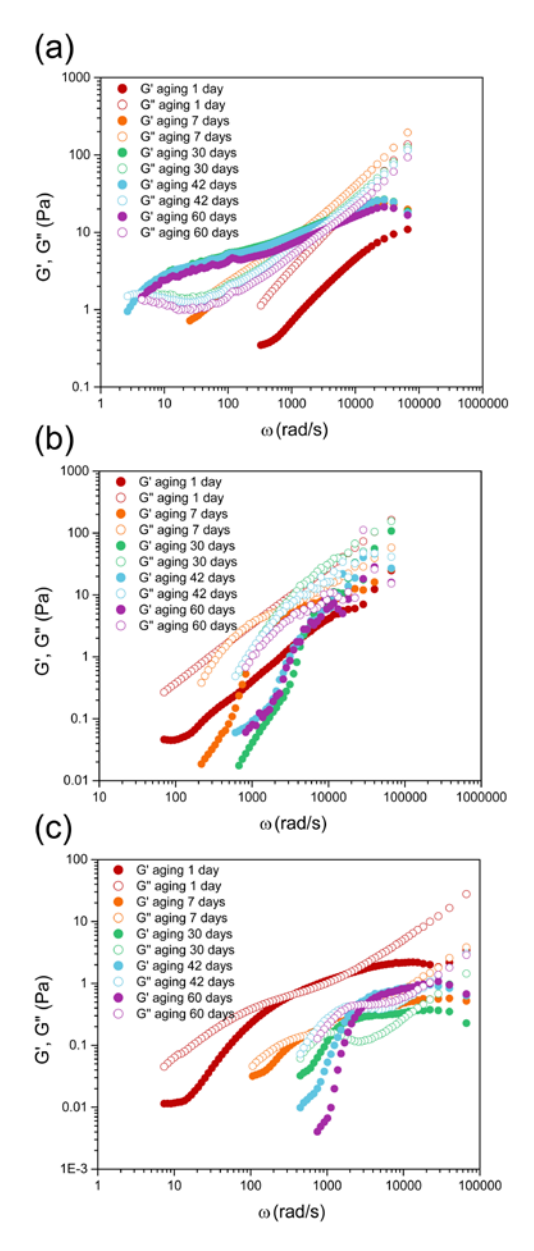
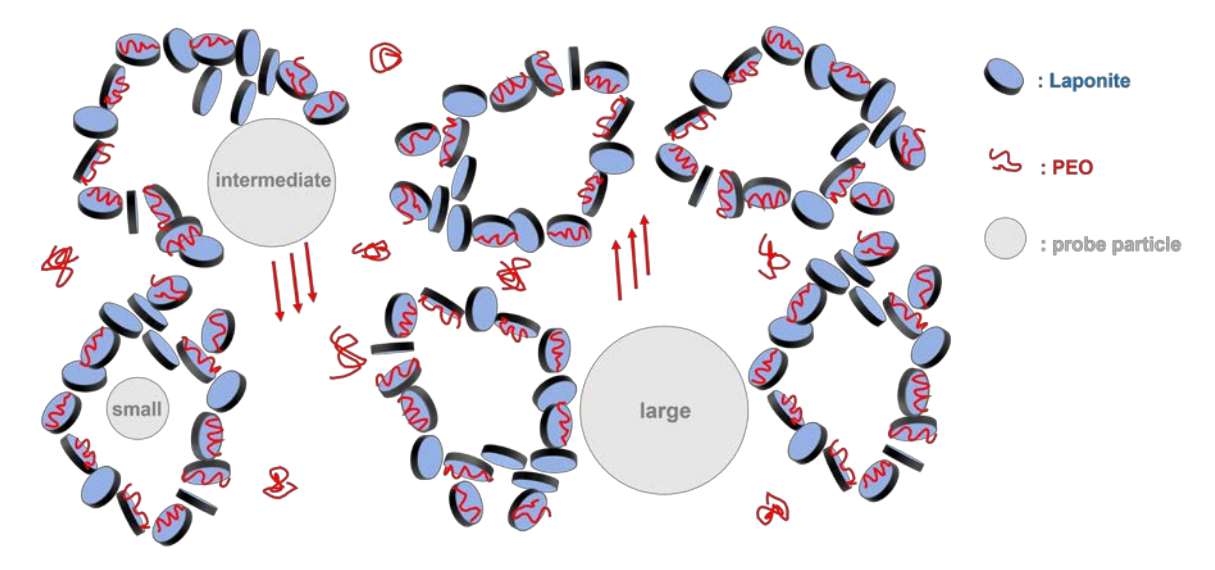


Figure 8. The storage modulus (filled circles) and loss modulus (open circles) calculated from the MSD data for L2PEO2.50 with different probe particle sizes at different aging times as indicated: (a) 65 nm, (b) 480 nm, and (c) 2000 nm.

To better elucidate the evolution of structure during the aging process, the viscoelastic properties of three representative samples with different PEO concentrations probed by different probe particles at various aging timing are reported in Figures 7, 8 and S2. Generally, for the 65 nm tracer in Figure 7, all samples display G' > G" in the intermediate frequency range with a minimum G" value after 7 days of aging, which conforms to the constrained regime reported by MSD with tracers trapped inside the local structure. To note, the change of storage modulus slows down over time compared to the change from 1

day to 7 days of aging and G' values become almost constant after 7 days. At late aging times, G' values are only weakly frequency-dependent as the structure develops more slowly within the aging duration, which indicates the formation of repulsive glass or gellike states. Specifically, the pure Laponite sample, as reported in our previous studies, turns into a repulsive glass structure within a short period and then the probed structure does not change much from 7 days to 60 days. The L2PEO1.25 and L2PEO2.50 samples show a similar evolution of viscoelastic properties upon aging in Figures 7b and 8a. Samples with the addition of PEO remain in a more liquid-like environment in the initial aging time and gradually transit to the gel-like state with G' eventually surpassing G". No significant changes are observed in the late aging time.

As for the medium and large size probe particles, the values of G' and G" become quite different even at the same aging time. For the Laponite sample in Figures S2a and S2c, both 480 nm and 2000 nm probe particles examine a more viscous environment with G" larger than G' at low frequency but G' values become close or slightly higher than G" values at high frequency. Although the low signal-to-noise ratio that leads to significant fluctuations at high frequency makes the trend of viscoelastic moduli incoherent, such a profile is consistent with the corresponding MSD data that has a curved trend at short lag time and then shows an upturn at long lag times, indicating escape from the arrested state. As for the Laponite/PEO samples in Figures S2b and 8b, 480 nm particle probed a similar microscale environment with that in the pure Laponite as the G" is dominant in the lower frequency range after 7 days. Instead like the pure Laponite sample, the polymer samples showed a different trend with the 2000 nm probe particle embedded as displayed in Figures S2d and 8c. For the 1 day of aging, G" is above G' in both low and high frequency ranges, while G' is slightly higher than G" at the intermediate frequency. Although the samples were still in a viscous liquid-like state, this indicates samples were experiencing particle rearrangements after 1 day of aging, which affected the motion of large probe particles. As the aging process proceeds, in the intermediate range of frequency, the G' values become higher than G" and showed a more gel-like local structure, suggesting that the probe particle was trapped after a short period of motion between the local structure after the rearrangement and it was able to escape the cage at large lag time. The viscoelastic moduli of all the samples probed by 65 nm probe particles at various aging time are also shown in Figure S3.



Scheme 1. Schematic illustration of the potential local structures probed by probe particles in microscale. Probe particles are not drawn to scale.

Based on our data, it is clear that the size of probe particle influences the measurement of viscoelastic properties in Laponite-polymer systems, providing different information at different length scales of local structures (Scheme 1). In our previous studies, it is found that the addition of free PEO chains induces a depletion attraction between the Laponite particles and leads to re-entrant behavior and a lower effective volume fraction, providing more available space.²⁹ In this case, the cage or aggregate size of Laponite and/or Laponite/polymer may decrease due to the induced interaction and the dynamic motion of tracers may be more easily affected when probing the surrounding environment. Considering the 65 nm probe particle, the relatively small size limits the length scale it can probe, and such tracers may only experience thermal motion inside the local structure and not get a chance to escape. Thus, a trend of the weakly-dependent storage modulus was observed after long aging times and the numerical value kept almost constant over time as the probe particle mainly explored the same surrounding structures. This is consistent with the MSD data, which tends to be flat at large lag times.

Similar viscoelastic results were obtained by 2000 nm tracers; large particles became arrested in the local medium. This may reveal that the cage size of Laponite/polymer network may be comparable to or slightly larger than the tracer, which provides limited space for the motion of large particles and thus hinders the escape of large particles. As for the 480 nm, this tracer could probe the local environment in the intermediate length scale and it may have the chance to escape if trapped in the surrounding cage. Once the tracers are able to escape the cage, they diffuse between the cage structures within the available space, and this makes them diffuse more like in a viscous state instead of an elastic state. In this way, different G' and G" information could be probed by the different probe particles due to the different length scales. This may also provide information about the cage size inside the sample. However, more quantitative experiments such as fluorescence

microscopy need to be conducted to confirm the actual size of cages and structural heterogeneities in these systems.

Although we must be careful not to over-interpret these MSD and microrheology data, it is clear that the probe particle size has a non-trivial effect on the microrheological measurements in these Laponite/polymer systems. The difference in the size of probe particles confers the different range scale they can probe, which also provides respective details about the heterogeneity of Laponite/polymer dispersion. More factors should also be considered in future investigations including the surface charge of probe particles, concentrations of Laponite dispersion, ionic strength and temperature, which may affect the thermal motion of tracers when inside the dispersion. To understand more about the evolution of colloid-polymer dispersion after aging, applying bulk rheology will be useful to explore the structural change in macroscale. By combining microrheology data, more details about re-entrant behavior or potential relationships between the probe particle and the colloid-polymer system may be obtained from microscale to macroscale. The DLSmicrorheology technique is limited to low concentration samples due to the issue of multiple scattering. Applying other kinds of microrheology techniques including Multiple Particle Tracking (MPT) and Optical Tweeters (OT) may help reduce the high noise in the measurement and display a consistent trend of structural rearrangement during the aging, which promotes the understanding of evolution of colloidal-polymer dispersion.

Conclusion

In conclusion, a series of Laponite/PEO samples were prepared and evaluated for their aging behavior using passive DLS-microrheology with various probe particle sizes. Two typical examples, pure Laponite and 1.50 wt% PEO with Laponite dispersion, were presented in detail to reveal the evolution of MSD curves and viscoelastic properties during the early aging process. After 1 day of aging, the probe particle size showed a significant effect on the MSD of samples containing PEO as compared to the neat Laponite samples. Higher concentrations of PEO showed a diffuse motion of small and medium size of probe particle with a logarithmic slope close to 1 throughout the frequency, while large probe particles displayed a typical three-regime behavior. As for the pure Laponite and lowest PEO concentration sample, both samples showed a non-linear MSD trend of small particles, suggesting the restricted motion of particles while the medium and large tracers experienced the retarded diffusion first followed by the superdiffusive motion due to the relaxation of constraints. By examining the factor $\langle \Delta r^2(\tau) \rangle a$, the cause of hindrance on the particle's motion was determined to cage trapping for most systems, rather than the local elasticity. At 7 days of aging, most samples displayed non-linear MSD curves due to the potential particle rearrangement except for the 2.50 wt% which remains in a viscous state. This implies the addition of homopolymer PEO could effectively influence and delay the transition to the arrested state. This is also verified by the changing of viscoelastic moduli of samples. The intermediate and large probe particles showed totally different MSD curves, suggesting the strong effect of probe particle sizes on the measurement. No

significant change in MSD data occurred after 30 days of aging. The corresponding evolution of loss modulus and storage modulus reveals the potential relationship between the tracer size and the cage size, though more experiments need to be carried out. This work provides some insights into the aging process of Laponite/PEO samples and reveals the significant effect of probe particle size on the microrheological measurements through DLS. Results may assist the understanding of the structural evolution of Laponite-polymer dispersion during the aging and may be useful in other structured colloid-polymer blended fluids or gels.

Supplementary Material

Mircorheology and mean-squared displacement (MSD) data for all samples and additional photos of samples.

Acknowledgments

Financial support for this work was provided by NSF awards CBET-1903189 and DGE-1922639. The sponsors had no role in the study design; in the collection, analysis and interpretation of data; in the writing of the report; and in the decision to submit the article for publication.

References

- 1. M. I. Carretero, Applied Clay Science 21, 155 (2002).
- 2. A. Usuki, N. Hasegawa, M. Kato and S. Kobayashi, Inorganic polymeric nanocomposites and membranes, 135 (2005).
- 3. T. Cosgrove, *Colloid science: principles, methods and applications.* (John Wiley & Sons, 2010).
- 4. E. Zaccarelli and W. C. Poon, Proceedings of the National Academy of Sciences **106**, 15203 (2009).
- 5. R. Angelini, E. Zaccarelli, F. A. de Melo Marques, M. Sztucki, A. Fluerasu, G. Ruocco and B. Ruzicka, Nat. Commun. **5**, 1 (2014).
- 6. H. Tanaka, J. Meunier and D. Bonn, Physical Review E 69, 031404 (2004).
- 7. D. Bonn, H. Tanaka, G. Wegdam, H. Kellay and J. Meunier, Europhys. Lett. **45**, 52 (1999).
- 8. A. S. Khair and J. F. Brady, J. Rheol. **52**, 165 (2008).
- 9. A. Shalkevich, A. Stradner, S. K. Bhat, F. Muller and P. Schurtenberger, Langmuir **23**, 3570 (2007).
- 10. S. Jabbari-Farouji, H. Tanaka, G. Wegdam and D. Bonn, Physical Review E **78**, 061405 (2008).
- 11. M. Pilavtepe, S. Recktenwald, R. Schuhmann, K. Emmerich and N. Willenbacher, J. Rheol. **62**, 593 (2018).
- 12. E. Tombacz and M. Szekeres, Applied clay science 27, 75 (2004).
- 13. P. Mongondry, J. F. Tassin and T. Nicolai, J. Colloid Interface Sci. **283**, 397 (2005).

- 14. S. L. Tawari, D. L. Koch and C. Cohen, J. Colloid Interface Sci. 240, 54 (2001).
- 15. B. Ruzicka and E. Zaccarelli, Soft Matter 7, 1268 (2011).
- 16. S. Jatav and Y. M. Joshi, Faraday Discuss. **186**, 199 (2016).
- 17. M. Pilavtepe, L. Delavernhe, A. Steudel, R. Schuhmann, N. Willenbacher and K. Emmerich, Clays Clay Miner. **66**, 339 (2018).
- 18. B. Zheng, J. R. Breton, R. S. Patel and S. R. Bhatia, Rheol. Acta **59**, 387 (2020).
- 19. S. Kishore, Y. Chen, P. Ravindra and S. R. Bhatia, Colloids Surf. A Physicochem. Eng. Asp. **482**, 585 (2015).
- 20. S. Kishore, S. Srivastava and S. R. Bhatia, Polymer **105**, 461 (2016).
- 21. K. Suman and Y. M. Joshi, Langmuir **34**, 13079 (2018).
- 22. S. Jabbari-Farouji, M. Atakhorrami, D. Mizuno, E. Eiser, G. Wegdam, F.
- MacKintosh, D. Bonn and C. Schmidt, Physical Review E 78, 061402 (2008).
- 23. D. Saha, R. Bandyopadhyay and Y. M. Joshi, Langmuir 31, 3012 (2015).
- 24. B. Ruzicka, L. Zulian and G. Ruocco, Langmuir **22**, 1106 (2006).
- 25. E. Loizou, P. Butler, L. Porcar, E. Kesselman, Y. Talmon, A. Dundigalla and G. Schmidt, Macromolecules **38**, 2047 (2005).
- 26. A. K. Atmuri and S. R. Bhatia, Langmuir **29**, 3179 (2013).
- 27. H. A. Baghdadi, E. C. Jensen, N. Easwar and S. R. Bhatia, Rheol. Acta 47, 121 (2008).
- 28. B. Zheng and S. R. Bhatia, Colloids Surf. A Physicochem. Eng. Asp. **520**, 729 (2017).
- 29. A. K. Atmuri, G. A. Peklaris, S. Kishore and S. R. Bhatia, Soft Matter **8**, 8965 (2012).
- 30. B. M. Vyas, A. V. Orpe, M. Kaushal and Y. M. Joshi, Soft Matter **12**, 8167 (2016).
- 31. J. P. Rich, G. H. McKinley and P. S. Doyle, J. Rheol. **55**, 273 (2011).
- 32. Q. Lu and M. J. Solomon, Physical Review E **66**, 061504 (2002).
- 33. N. Yang, J. L. Hutter and J. R. de Bruyn, J. Rheol. **56**, 797 (2012).
- 34. T. G. Mason, Rheol. Acta **39**, 371 (2000).
- 35. B. J. Landrum, W. B. Russel and R. N. Zia, J. Rheol. **60**, 783 (2016).
- 36. T. Van De Laar, R. Higler, K. Schroën and J. Sprakel, Scientific Reports **6**, 1 (2016).
- 37. P. Mongondry, T. Nicolai and J.-F. Tassin, J. Colloid Interface Sci. **275**, 191 (2004).
- 38. S. Kawaguchi, G. Imai, J. Suzuki, A. Miyahara, T. Kitano and K. Ito, Polymer 38, 2885 (1997).
- 39. N. Ziębacz, S. A. Wieczorek, T. Kalwarczyk, M. Fiałkowski and R. Hołyst, Soft Matter 7, 7181 (2011).
- 40. C. Lian, Z. Lin, T. Wang, W. Sun, X. Liu and Z. Tong, Macromolecules **45**, 7220 (2012).
- 41. E. Paineau, I. Bihannic, C. Baravian, A.-M. Philippe, P. Davidson, P. Levitz, S. S. Funari, C. Rochas and L. J. Michot, Langmuir **27**, 5562 (2011).
- 42. H. A. Baghdadi, H. Sardinha and S. R. Bhatia, Journal of Polymer Science Part B: Polymer Physics **43**, 233 (2005).
- 43. K. S. Breuer, *Microscale diagnostic techniques*. (Springer, 2005).
- 44. T. G. Mason and D. A. Weitz, Phys. Rev. Lett. **74**, 1250 (1995).